

Numerical and approximate analytical results for the frustrated spin- 1/2 quantum spin chain

This content has been downloaded from IOPscience. Please scroll down to see the full text.

1995 J. Phys.: Condens. Matter 7 8605

(<http://iopscience.iop.org/0953-8984/7/45/016>)

View [the table of contents for this issue](#), or go to the [journal homepage](#) for more

Download details:

IP Address: 130.133.8.114

This content was downloaded on 22/05/2017 at 11:38

Please note that [terms and conditions apply](#).

You may also be interested in:

[A coupled-cluster treatment of spin- 1/2 systems with nearest- and next-nearest-neighbour interactions](#)

D J J Farnell and J B Parkinson

[Density matrix renormalization group study of the correlation function of the bilinear-biquadratic spin-1 chain](#)

R J Bursill, T Xiang and G A Gehring

[The spin-one Heisenberg-biquadratic quantum spin chain treated by the coupled-cluster method](#)

R F Bishop, J B Parkinson and Yang Xian

[A microscopic approach to the dimerization in frustrated spin- 1/2 antiferromagnetic chains](#)

Y Xian

[The density matrix renormalization group and critical phenomena](#)

R J Bursill and F Gode

[An application of the coupled-cluster method to the S= 1/2 triangular-lattice antiferromagnet](#)

Chen Zeng, I Staples and R F Bishop

Numerical and approximate analytical results for the frustrated spin- $\frac{1}{2}$ quantum spin chain

R Bursill[†], G A Gehring[†], D J J Farnell[‡], J B Parkinson[‡], Tao Xiang^{†§} and Chen Zeng[‡]

[†] Department of Physics, University of Sheffield, Sheffield S3 7RH, UK

[‡] Department of Mathematics, UMIST, PO Box 88, Manchester M60 1QD, UK

Received 27 July 1995

Abstract. We study the $T = 0$ frustrated phase of the 1D quantum spin- $\frac{1}{2}$ system with nearest-neighbour and next-nearest-neighbour isotropic exchange known as the Majumdar–Ghosh Hamiltonian. We first apply the coupled-cluster method of quantum many-body theory based on a spiral model state to obtain the ground-state energy and the pitch angle. These results are compared with accurate numerical results using the density matrix renormalization group method, which also gives the correlation functions. We also investigate the periodicity of the phase using the Marshall sign criterion. We discuss particularly the behaviour close to the phase transitions at each end of the frustrated phase.

1. Introduction

There is currently much interest in quantum spin systems that exhibit frustration. This has been stimulated in particular by the work on the magnetic properties of the cuprates which become high- T_c superconductors when doped. The frustration in these 2D materials arises because of antiferromagnetic exchange across the diagonals of the squares as well as along the edges. Other 2D frustrated systems are the triangular and Kagomé lattices.

In this paper we study a simple 1D spin system which is also frustrated for some range of its parameters. This is a spin-1/2 model with isotropic nearest- and next-nearest-neighbour exchange given by

$$\mathcal{H} = \cos \omega \sum_l \mathbf{s}_l \cdot \mathbf{s}_{l+1} + \sin \omega \sum_l \mathbf{s}_l \cdot \mathbf{s}_{l+2} \quad (1.1)$$

where the sum over l is over all N atoms with periodic boundary conditions. We shall also use the notation $J_1 = \cos \omega$ and $J_2 = \sin \omega$.

The $T = 0$ phase diagram of this model is given in figure 1. The antiferromagnetic (AF) phase extends over the region $-\pi/2 < \omega < \omega_{\text{MG}}$, where $\omega_{\text{MG}} = \tan^{-1}(1/2)$. The point ω_{MG} is the Majumdar–Ghosh (MG) Hamiltonian (Majumdar and Ghosh 1969a, b; see also Haldane 1982) at which the ground state consists of dimerized singlets with a gap to the excited states. In a recent paper by two of the present authors (Zeng and Parkinson 1995), a dimer variational wavefunction was proposed which is exact at ω_{MG} and gives good results for a large range around this point.

[§] Present address: IRC in Superconductivity, University of Cambridge, Madingley Road, Cambridge CB3 0HE, UK.

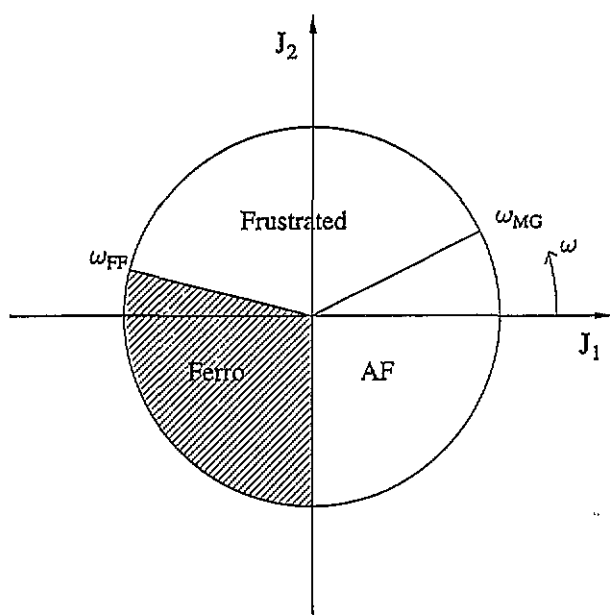


Figure 1. $T = 0$ phase diagram of the model.

Much of the recent work on this system has focused on the transition from a gapless 'spin-liquid' state which is known exactly at $\omega = 0$, to a dimerized regime with a gap which is also known exactly at $\omega = \omega_{MG}$. The transition occurs at $J_2/J_1 = 0.2411(1)$ ($\omega = 0.2366(1)$ (Okamoto and Nomura 1992)). The same authors have also studied the phase diagram in the vicinity of this transition in the anisotropic version of this model (Nomura and Okamoto 1993, 1994).

The frustrated regime is given by $\omega_{MG} < \omega < \omega_{FF}$, where $\omega_{FF} = \tan^{-1}(-1/4) = 3.3865$ is the point at which a first-order transition to a ferromagnetic regime occurs. This was first studied numerically by Tonegawa and Harada (1987) who found evidence of change in the position of the peak of the correlation function as a function of ω . Here we shall use a variety of methods to investigate the whole of the frustrated regime, including $\omega > \pi/2$.

It will be useful to compare our results with those of the classical Hamiltonian. In this regime the minimum classical energy is obtained by forming a spiral with a pitch angle θ between neighbouring spins, where $\theta = \cos^{-1}(-J_1/4J_2)$. The classical boundary with the AF phase is at $\omega_C = \tan^{-1}(1/4) = 0.2450$. The real-space periodicity thus increases monotonically from two at the AF boundary to infinity at the ferromagnetic boundary.

2. The CCM formalism

In a recent paper (Farnell and Parkinson 1994, hereinafter referred to as I), the coupled-cluster method (CCM) was applied by two of the present authors to the antiferromagnetic (AF) phase. For a description of the CCM applied to spin systems see Bishop *et al* (1991) and the references in I. In the AF phase the natural choice of a model state for the CCM is the Néel state used in I.

For the frustrated regime, however, this model state is physically unrealistic and the CCM based upon it gives poor results. One possible choice is suggested by the fact that when $\omega = \pi/2$ we have $J_1 = 0$ and $J_2 = 1$, so the Hamiltonian (1.1) describes two uncoupled antiferromagnetic Heisenberg chains. At this point a 'double-Néel' model state

with a periodicity of four unit cells would be appropriate and would lead to precisely the same results as for the single chain ($J_1 = 1, J_2 = 0$) with suitable scaling factors. We did carry out CCM calculations based on this model state and obtained reasonable results for a range of ω around $\pi/2$. These results will be described briefly later.

Another possible model state is suggested by the classical ground state in this regime. For this reason we have performed CCM calculations based on a spiral model state in which the pitch angle θ is taken as a variational parameter. A necessary condition to perform CCM calculations is the existence of a complete set of mutually commuting creation operators so that an arbitrary state of the system can be constructed starting from the model state. We obtain these as follows.

The spiral model state is taken to have all spins aligned in the XZ plane with the n th spin making an angle $n\theta$ with the Z axis. We then introduce local axes such that each atom is in the quantum spin state $|-\rangle$. We use the usual notation $|\pm\rangle$ for the states with eigenvalues of s^z equal to $\pm\frac{1}{2}$. Using the local axes the Hamiltonian (1.1) becomes

$$\begin{aligned} \mathcal{H} = J_1/4 \sum_i \{ & [\cos(\theta) - 1](s_i^- s_{i+1}^- + s_i^+ s_{i+1}^+) + [\cos(\theta) + 1](s_i^- s_{i+1}^+ + s_i^+ s_{i+1}^-) \\ & + 2 \sin(\theta)(s_i^- + s_i^+)(s_{i+1}^z - s_{i-1}^z) + 4 \cos(\theta)s_i^z s_{i+1}^z \} \\ & + J_2/4 \sum_i \{ [\cos(2\theta) - 1](s_i^- s_{i+2}^- + s_i^+ s_{i+2}^+) + [\cos(2\theta) + 1](s_i^- s_{i+2}^+ + s_i^+ s_{i+2}^-) \\ & + 2 \sin(2\theta)(s_i^- + s_i^+)(s_{i+2}^z - s_{i-2}^z) + 4 \cos(2\theta)s_i^z s_{i+2}^z \}. \end{aligned} \quad (2.1)$$

This equation contains terms which have an odd number of spin-flips multiplied by a coefficient $\sin(\theta)$ or $\sin(2\theta)$. By symmetry the ground-state energy E_g will be an even function of θ , which suggests that these terms should not contribute to E_g . We have confirmed explicitly that this is correct for the CCM approximation scheme described in the following section, and for clarity we shall omit these terms from \mathcal{H} from now on.

2.1. Approximation schemes

We shall work with Pauli spin operators σ_i^α , related to the spin angular momentum operators in the usual way: $\sigma_i^\alpha = 2s_i^\alpha$, $\alpha = x, y, z$ and $\sigma_i^\pm = \frac{1}{2}(\sigma_i^x \pm i\sigma_i^y)$. These definitions apply to all sites as there is no partition into different sublattices in this scheme. The Hamiltonian of (1.1) becomes

$$\begin{aligned} \mathcal{H} = J_1/4 \sum_i \{ & [\cos(\theta) - 1](\sigma_i^- \sigma_{i+1}^- + \sigma_i^+ \sigma_{i+1}^+) + [\cos(\theta) + 1](\sigma_i^- \sigma_{i+1}^+ + \sigma_i^+ \sigma_{i+1}^-) \\ & + \cos(\theta)\sigma_i^z \sigma_{i+1}^z \} + J_2/4 \sum_i \{ [\cos(2\theta) - 1](\sigma_i^- \sigma_{i+2}^- + \sigma_i^+ \sigma_{i+2}^+) \\ & + [\cos(2\theta) + 1](\sigma_i^- \sigma_{i+2}^+ + \sigma_i^+ \sigma_{i+2}^-) + \cos(2\theta)\sigma_i^z \sigma_{i+2}^z \}. \end{aligned} \quad (2.2)$$

In the CCM the true ground state is written

$$|\Psi\rangle = e^S |\Phi\rangle. \quad (2.3)$$

The CCM correlation operator S is constructed entirely out of creation operators with respect to the model state, i.e. a linear combination of all possible C_I^+ , where each C_I^+ is a product of creation operators from $\{\sigma_i^+\}$ consistent with the conserved quantities. The Hamiltonian of (2.2) contains only terms that involve an even number of spin flips. This means that all

terms in e^S and hence in S should only involve even numbers of σ^+ operators. Note that this would not be true had the $\sin(\theta)$ and $\sin(2\theta)$ terms not been neglected, and this point is considered further below.

We shall use the following approximation schemes, all of which were described in I.

(i) Full SUB2. In this scheme S includes all possible products of two spin-flip operators:

$$S = \frac{1}{2} \sum_i \sum_r b_r \sigma_i^+ \sigma_{i+r}^+ \quad (2.4)$$

where i runs over all N sites and r is an integer with $|r| \leq N/2$. By symmetry $b_{-r} = b_r$.

(ii) SUB2-3. This is a subset of full SUB2 in which all b_r are set to zero except $b_{\pm 1}$ and $b_{\pm 2}$:

$$S = b_1 \sum_i \sigma_i^+ \sigma_{i+1}^+ + b_2 \sum_i \sigma_i^+ \sigma_{i+2}^+. \quad (2.5)$$

Using the same notation \sim as in I, we calculate the similarity transform with respect to S of the spin operators. For example

$$\tilde{\sigma}_i^+ = e^{-S} \sigma_i^+ e^S. \quad (2.6)$$

Using these the transformed Hamiltonian $\tilde{\mathcal{H}}$ can be obtained. Operating on the ground-state Schrödinger equation

$$\tilde{\mathcal{H}}|\Phi\rangle = E_g|\Phi\rangle \quad (2.7)$$

with $\langle\Phi|$ then gives the following equation for the ground-state energy per spin in either approximation as

$$E_g/N = J_1/4\{\cos(\theta) + [\cos(\theta) - 1]b_1\} + J_2/4\{\cos(2\theta) + [\cos(2\theta) - 1]b_2\}. \quad (2.8)$$

To find b_1 and b_2 we obtain a set of coupled non-linear equations for the coefficients retained in each of the approximation schemes by operating on (2.7) with $\langle\Phi|C_I$, where C_I is the Hermitian conjugate of one of the strings of creation operators (combinations of σ_i^+) present in S .

Lastly in this section we note that if odd numbers of spin flips had been allowed there would be a term in S of the form $a \sum_i \sigma_i^+$. We have performed calculations in the SUB2-3 approximation in which the extra $\sin(\theta)$ and $\sin(2\theta)$ terms were retained in the Hamiltonian. In this case $a = 0$ is the only physically reasonable solution, and the extra terms give zero contribution to the ground-state energy.

3. The coupled non-linear equations

Using the S given by (2.4), we operate on (2.7) with $\sum_i \sigma_i^- \sigma_{i+\rho}^-$, and obtain the full SUB2 equations:

$$\begin{aligned} J_1 \sum_{\rho} (1 - \delta_{\rho,0}) & \left(A_1 \delta_{\rho,\rho} + B_1 b_{\rho} + 2[\cos(\theta) + 1]b_{\rho+\rho} + [\cos(\theta) - 1] \sum_s b_{\rho+s+\rho} b_s \right) \\ & + J_2 \sum_{\delta} (1 - \delta_{\delta,0}) \left(A_2 \delta_{\delta,\delta} + B_2 b_{\delta} \right. \\ & \left. + 2[\cos(2\theta) + 1]b_{\delta+\rho} + [\cos(2\theta) - 1] \sum_s b_{\delta+s+\delta} b_s \right) = 0 \end{aligned} \quad (3.1)$$

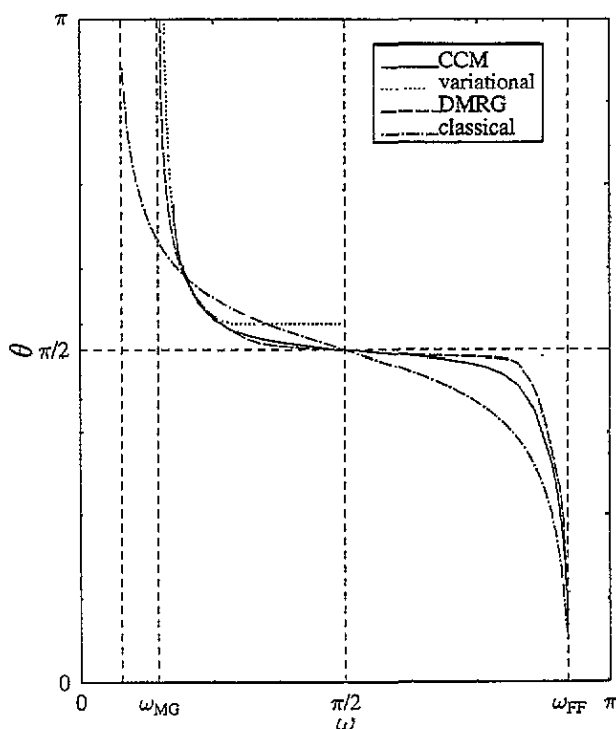


Figure 2. Pitch angle θ as a function of ω obtained by various methods.

where

$$A_1 = [\cos(\theta) - 1](1 + 2b_1^2) + 4b_1 \cos(\theta) \quad (3.2a)$$

$$A_2 = [\cos(2\theta) - 1](1 + 2b_2^2) + 4b_2 \cos(2\theta) \quad (3.2b)$$

$$B_1 = -4 \cos(\theta) + 4[1 - \cos(\theta)]b_1 \quad (3.3a)$$

$$B_2 = -4 \cos(2\theta) + 4[1 - \cos(2\theta)]b_2 \quad (3.3b)$$

with $\rho = \pm 1$, $\delta = \pm 2$ and s is any positive or negative integer. The solution of (3.1) is given in section 4.

For the SUB2-3 approximation scheme (3.1) reduces to the pair of coupled non-linear equations

$$J_1\{[\cos(\theta) - 1](1 + 2b_2^2 - 3b_1^2) - 4b_1 \cos(\theta) + 2b_2[\cos(\theta) + 1]\} \\ + J_2\{[1 - \cos(2\theta)]4b_1b_2 - 8b_1 \cos(2\theta) + 2b_1[\cos(2\theta) + 1]\} = 0 \quad (3.4)$$

and

$$J_1\{[1 - \cos(\theta)]4b_1b_2 - 8b_2 \cos(\theta) + 2b_1[\cos(\theta) + 1]\} \\ + J_2\{[\cos(2\theta) - 1](1 + 2b_1^2 - 3b_2^2) - 4b_2 \cos(2\theta)\} = 0. \quad (3.5)$$

Equations (3.4) and (3.5) can be solved numerically and hence E_g/N obtained in the SUB2-3 approximation for a given θ . Finally, θ is varied to find a minimum value for E_g/N .

The results for θ as a function of ω are shown in figure 2. We observe that the value of θ obtained by this method remains close to $\pi/2$ over a much wider range of ω than in the classical calculation. We mentioned earlier that calculations based on a 'double-Néel' model state have been carried out. As can now be easily understood, the results were in good agreement with the ones based on the spiral model state over quite a wide range of ω around $\pi/2$.

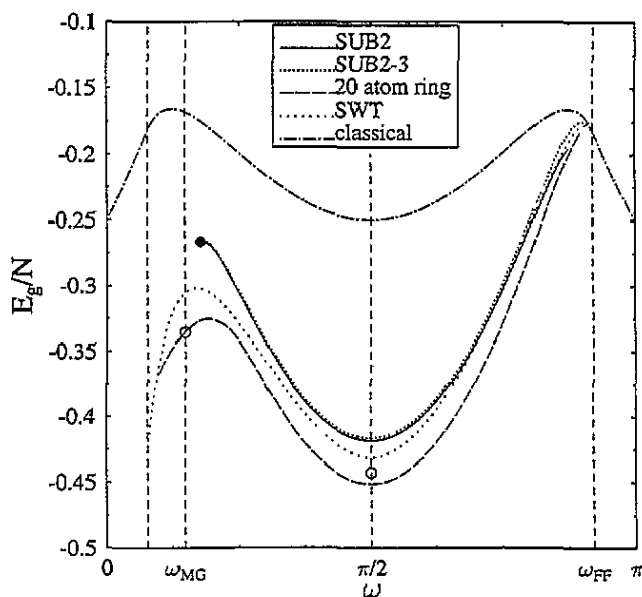


Figure 3. Ground-state energy per spin as a function of ω . Open circles are exact results. The full circle is the CCM terminating point.

The results for the ground-state energy per spin are shown in figure 3 and are compared with the values obtained by direct diagonalization of a chain of 20 spins, the results of spin-wave theory (SWT), and also with a 'classical' result which is the expectation value of the Hamiltonian in the classical ground state. The exact results at $\omega = \omega_{MG}$ and $\omega = \pi$ are also marked on this figure.

The full SUB2 equations can be solved numerically by first performing a Fourier transform, as in I. Details are given in appendix 1. The results are similar to the SUB2-3 results and are also shown in the figure. Both SUB2 and SUB2-3 have a 'terminating point' at which the spiral solution ceases to exist. The terminating point for SUB2 is shown on figure 3.

4. DMRG study of the periodicity

We next turn to the density matrix renormalization group (DMRG) method in order to perform a numerical study of the periodicity that can be compared with the CCM results discussed above. We achieve this by accurately calculating the position of the peak of the Fourier-transformed ground-state correlation function (Bursill *et al* 1995).

4.1. The DMRG method

The DMRG was introduced in a series of papers by White and co-workers (White and Noack 1992, White 1992, 1993) and a highly successful application to the spin-1 antiferromagnetic chain (White and Huse 1993) established the DMRG as the method of choice for studying the low-energy physics of quantum lattice systems in one dimension. White (1993) describes in great detail efficient algorithms for calculating low-lying energies and correlation functions of spin chains, so we will only briefly describe the method here. We restrict our discussion to the infinite lattice algorithm (White 1993) which was used in our calculations.

The DMRG is an iterative truncated basis procedure whereby a large chain (or superblock) is built up from a single site by adding a small number of sites at a time. At each stage the superblock consists of system and environment blocks (determined from previous iterations) in addition to a small number of extra sites. Also determined from previous iterations are the matrix elements of various operators such as the block Hamiltonians and the spin operators for the sites (at the end(s) of the blocks) with respect to a truncated basis. Tensor products of the states of the system block, the environment block and the extra sites are then formed to provide a truncated basis for the superblock. The ground state $|\psi\rangle$ (or other targeted state) of the superblock is determined by a sparse matrix diagonalization algorithm.

At this point, correlation functions, local energies and other expectation values are calculated with respect to $|\psi\rangle$. Next, a basis for an augmented block, consisting of the system block and a specified choice of the extra sites, is formed from tensor products of system block and site states. The augmented block becomes the system block in the next iteration. However, in order to keep the size of the superblock basis from growing, the basis for the augmented block is truncated. We form a density matrix by projecting $|\psi\rangle\langle\psi|$ onto the augmented block which we diagonalize with a dense matrix routine. We retain the *most probable* eigenstates (those with the largest eigenvalues) of the density matrix in order to form a truncated basis for the augmented block that is around the same size as the system block basis. Matrix elements for the Hamiltonian and active site operators, together with any other operators that are required for, say, correlation functions are then updated.

The environment block used for the next iteration is usually chosen to be a reflected version of the system block. The initial system and environment blocks are chosen to be single sites.

The accuracy and computer requirements of the scheme is fixed by n_s , the number of states retained per block (of good quantum numbers) at each iteration; n_s determines the truncation error, which is the sum of the eigenvalues of the density matrix corresponding to states which are shed in the truncation process. The error in quantities such as the ground-state energy scale linearly with the truncation error (White and Huse 1993).

4.2. Application of the DMRG to the frustrated spin-1/2 chain

We have applied the infinite lattice DMRG algorithm to (1.1) using a number of superblock configurations and boundary conditions. All the interactions (intra-block, inter-block and superblock Hamiltonians) commute with the total z spin $S_T^z \equiv \sum_i S_i^z$, so S_T^z is a good quantum number which can be used to block diagonalize the system, environment and super blocks. For even numbers of sites, the ground state of the superblock $|\psi\rangle$ is a singlet with zero total spin so we only need to consider superblock states with $S_T^z = 0$. We found that the most CPU efficient configuration was the standard open ended superblock of the form system-site-site-environment (White 1993).

As mentioned, in applying the DMRG to (1.1), we are concerned with the correlation function

$$C_{jl} \equiv \langle S_j^z S_l^z \rangle \quad (4.1)$$

and hence its Fourier transform

$$\tilde{C}(q) = \frac{1}{V} \sum_{jl} C_{jl} e^{iq(j-l)}. \quad (4.2)$$

We are particularly interested in q^* , the value of q where $\tilde{C}(q)$ has its peak. This leads to a natural (working) identification of the ground-state periodicity with $2\pi/q^*$ which was given in (Bursill *et al* 1995) where another frustrated spin model, the spin-1 model with bilinear and biquadratic exchange, was studied.

In practice, C_{jl} is calculated with j and l approximately equidistant from the centre of the superblock and far from the ends of the block so as to avoid end effects. In forming $\tilde{C}(q)$ we calculate C_{jl} for $0 \leq |j-l| \leq 60$. The algorithm is iterated until these quantities converge. We test the algorithm by exactly calculating C_{jl} for finite chains of up to 20 sites using the Lanczos method and ensuring that these results are reproduced by the DMRG.

Bursill *et al* (1995) noted that there are two impediments to an accurate calculation of (4.2). Firstly, for given j and l , we must have n_s sufficiently large that C_{jl} is accurately determined. Secondly, for given q , we must retain enough accurately calculated C_{jl} in truncating the infinite series to ensure an accurate result. It was found (Bursill *et al* 1995) that if the system has a significant energy gap and exponentially decaying correlation functions with a short correlation length, then the C_{jl} converge rapidly with n_s and the Fourier series converges very rapidly. On the other hand, in critical or near-critical regions where the energy gap is small or zero and the correlation functions decay algebraically or have a large correlation length then convergence is very slow.

By choosing n_s up to 90, it is found that the main source of inaccuracy in calculating $\tilde{C}(q)$ in these regions is Fourier series truncation. We plot $\tilde{C}(q)$ as a function of q for various values of J_2/J_1 in figure 4.

As mentioned, it was determined using exact diagonalization and finite-size scaling methods (Okamoto and Nomura 1992) that the model is critical (gapless with algebraically decaying correlation functions) for $0 \leq J_2/J_1 \leq \tan \omega_c$ and gapped beyond this region where $\tan \omega_c = 0.2411(1)$. Correspondingly, we find that $\tilde{C}(q)$ converges slowly and has oscillation due to Fourier series truncation in and around the critical region. In the region $0.3 \leq J_2/J_1 \leq 2$ we find that $\tilde{C}(q)$ converges rapidly to a smooth function.

Now at the extreme point where $J_1 = 0$ we have two decoupled Heisenberg chains and so C_{jl} vanishes if j and l lie on different sublattices but C_{jl} decays algebraically on a given sublattice. We in fact find that $\tilde{C}(q)$ converges slowly for $J_2/J_1 \geq 2.5$, indicating that there may be a finite interval around the $J_1 = 0$ point where the model is critical.

We next turn to the question of periodicity in the ground state. As mentioned, we define the periodicity in terms of the position q^* at which $\tilde{C}(q)$ has its peak. A plot of q^* as a function of ω is included in figure 2. We see that the simple analytical CCM result for the pitch angle improves dramatically upon the classical result. Also, we see that the dimer variational wavefunction (Zeng and Parkinson 1995) gives an excellent estimate of the pitch angle in a region to the right of the solvable point.

q^* converges very rapidly with n_F (the number of Fourier coefficients used in forming (4.2)) and n_s in the region $0.3 < J_2/J_1 < 2$ and we can accurately determine the threshold

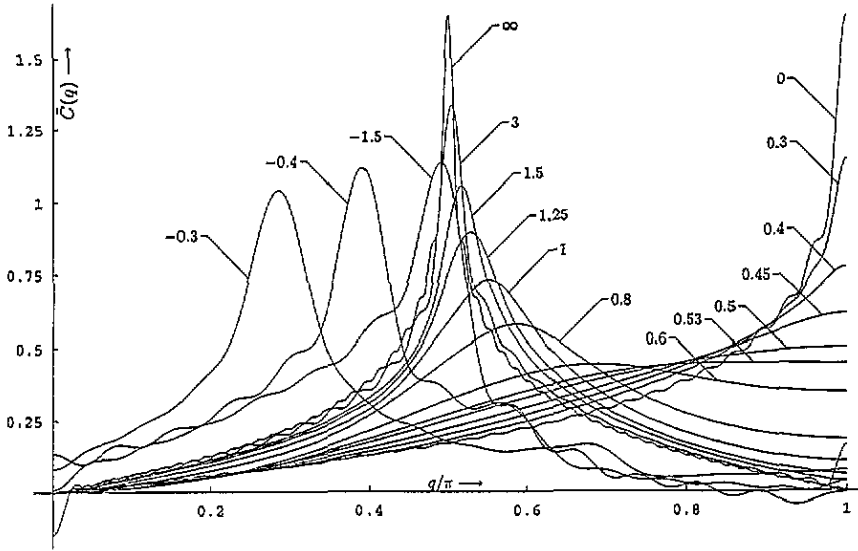


Figure 4. Fourier-transformed correlation functions for various values of J_2/J_1 obtained from the DMRG.

(the onset of the spiral phase) $\tilde{\omega}$ at which q^* begins to move away from π (as the periodicity begins to change from 2 to 4). Such a threshold was found in (Bursill *et al* 1995) as the biquadratic interaction was increased relative to the bilinear interaction. Again, q^* could be accurately determined near the threshold. Using the same analysis as in Bursill *et al* (1995), we find

$$\tan \tilde{\omega} = 0.52063(6). \quad (4.3)$$

This is to be compared with the classical threshold (0.25) and the terminating point from the CCM theory (0.623).

In a recent preprint, Chitra *et al* (1994) have studied the extension of (1.1) where there is also dimerization δ such that nearest-neighbour exchange carries a factor of $1 + \delta$ and $1 - \delta$ on successive bonds. They conjectured that there is a disorder line given by $J_2/J_1 = \frac{1}{2}(1 - \delta)$ such that, in the δ - J_2/J_1 plane, the structure factor has its peak at π below the line and decreases from π to $\pi/2$ as J_2/J_1 is increased above the line. In the case (1.1) of no dimerization ($\delta = 0$) gives $\tan \tilde{\omega} = 1/2$ (i.e. the threshold is the exactly solvable point).

Now at the solvable point the ground state is a perfect dimer where spins form a singlet with their dimer pair but are otherwise uncorrelated. The correlation function is

$$C_{ij} = \begin{cases} \frac{1}{4} & i = j \\ -\frac{1}{4} & i \text{ and } j \text{ on the same dimer} \\ 0 & \text{otherwise.} \end{cases}$$

The Fourier transform is therefore

$$\tilde{C}(q) = \frac{1}{4}(1 - \cos q) \quad (4.4)$$

whence $\tilde{C}''(\pi) = -1/4 \neq 0$ so, unless $\tilde{C}''(\pi)$ is highly singular at the threshold, the threshold (i.e. the point where $\tilde{C}''(\pi)$ vanishes) cannot occur at the solvable point. This is borne out by our result (4.3).

4.3. Further interpretation of the spiral phase

We have defined the ground-state periodicity and the spiral phase ($\tilde{\omega}$) in terms of the peak position of the Fourier-transformed correlation function. It has, however been shown (Schollwöck *et al* 1995) that further insight into disorder and incommensurate spin distortions in the ground state can be gained by investigating the correlation function in real space. In table 1 we list the correlation function in real space $C(r)$ for $J_2/J_1 = 0.49, 0.5$ (the solvable point), 0.51 and 0.5206... (the threshold). (As we shall see, in the gapped region, the ground state has broken translational symmetry and $C(r)$ is defined to be the average of C_{j+j+r} over a number of the sites j in the middle of the chain).

Table 1. Correlation function in real space $C(r)$ for various values of J_2/J_1 obtained from the DMRG.

r	0.49	0.5	0.51	$\tan \tilde{\omega}$
0	0.25	0.25	0.25	0.25
1	-0.127	-0.125	-0.123	-0.121
2	0.00386	0	-0.0039	-0.00806
3	-0.00237	0	0.00234	0.00477
4	0.000892	0	-0.000764	-0.00143
5	-0.000571	0	0.000425	0.000714
6	0.00022	0	-0.000119	-0.000145

We see that modulations begin to appear for J_2/J_1 values between the solvable point and the threshold where $C(2)$ changes sign, i.e. the Majumdar–Ghosh point is a disorder point, separating phases of commensurate and incommensurate correlations (in real space). Following Schollwöck *et al* (1995), the threshold $\tilde{\omega}$, where incommensurate spin oscillations would begin to be observed (experimentally) in the structure factor, is identified as a Lifshitz point. We would expect that in the limit of large spin S , the classical disorder point, the quantum disorder point and the Lifshitz point would merge, there being a single point separating commensurate and incommensurate phases both in terms of real and momentum space.

4.4. Translational symmetry breaking in the ground state—a dimer order parameter

As mentioned above, Okamoto and Nomura (1992) calculated the critical point $\tan \omega_c = 0.2411(1)$ separating gapped from gapless phases. Chitra *et al* (1994) calculated the energy gap using the DMRG and deduced $\tan \omega_c = 0.298(1)$, a result which is incompatible with that of Okamoto and Nomura (1992). It is, however, known (White 1993, Bursill *et al* 1995, Schollwöck *et al* 1995) that it is difficult to obtain accurate energies with the DMRG for critical or near-critical systems. This is again borne out when we apply the DMRG to the calculation of another order parameter that characterizes this phase transition.

It is known that the ground state for the Heisenberg model $J_2 = 0$ has no symmetry breaking whereas at the Majumdar–Ghosh point $J_2 = J_1/2$ the ground state has broken translational symmetry, the correlator $C_{j,j+1}$ equating to 0 and $-1/4$ on successive bonds $(j, j+1)$. To measure this broken symmetry, we define a dimer order parameter D by

$$D(N) \equiv |C_{N/2-1, N/2} - C_{N/2, N/2+1}| \quad (4.5)$$

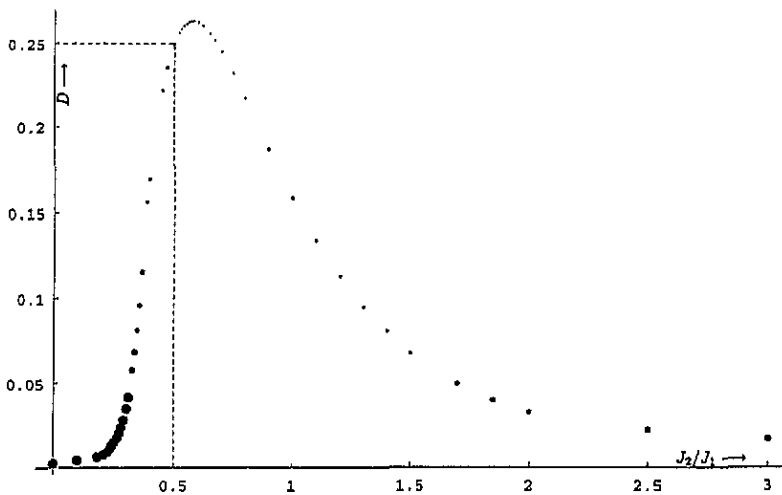


Figure 5. Dimer order parameter D as a function of J_2/J_1 obtained from the DMRG.

and $D \equiv \lim_{N \rightarrow \infty} D(N)$, where N is the size of an even open chain.

$D(N)$ converges very slowly in and around the critical region $0 \leq J_2/J_1 < 0.35$ and rapidly (with respect to both N and n_s) around the threshold $0.45 \leq J_2/J_1 < 1$. A plot of D against J_2/J_1 for $n_s = 40$ is given in figure 5. We note that D is maximal at around $J_2/J_1 \approx 0.58$, i.e. neither the disorder point (0.5) nor the Lifshitz point (0.52...). The fact that D exceeds $1/4$ to the right of the disorder point is indicative of the incommensurate oscillations whereby the values of $C_{j,j+1}$ on successive bonds ($j, j+1$) can have opposite sign. We see that the critical point is not well defined and only qualitative information about the phase transition can be deduced from this procedure. We shall attempt to address the question of how the DMRG can be adapted to study critical phenomena in future publications.

5. The Marshall sign results

An additional method of studying the periodicity of the ground state in the frustrated phase is by means of the Marshall–Peierls (Marshall 1955) sign criterion. Preliminary results were reported in an earlier paper (Zeng and Parkinson 1995) so a detailed description will not be given here. We have now obtained results for an open chain of 16 atoms and these confirm and extend those of shorter chains.

In figure 6 we show the parameter ρ_i for $i = 1, 2, 3, 4$, corresponding to a periodicity of $2i$ in the 16 atom chain. This parameter will be close to 1 if the ground state ‘conforms’ to the given periodicity and will be close to 0.5 if the conformity is poor. The main features are as follows.

For ω in the range $0 \leq \omega \leq \omega_{\text{MG}}$ (outside the frustrated regime) ρ_1 is very close to 1. For $\omega_{\text{MG}} \leq \omega$ there is an extended region in which ρ_2 is closest to 1. An interesting and totally unexplained feature is the shallow double minimum in the value of ρ_2 for ω near $\pi/4$, which was also observed for shorter chains. At $\omega \approx 2.74$ there is a smooth crossover to a state in which ρ_3 is largest and finally a more complicated behaviour as ω approaches ω_{FF} . An enlarged picture of the latter region is shown in figure 7. The sharp changes in

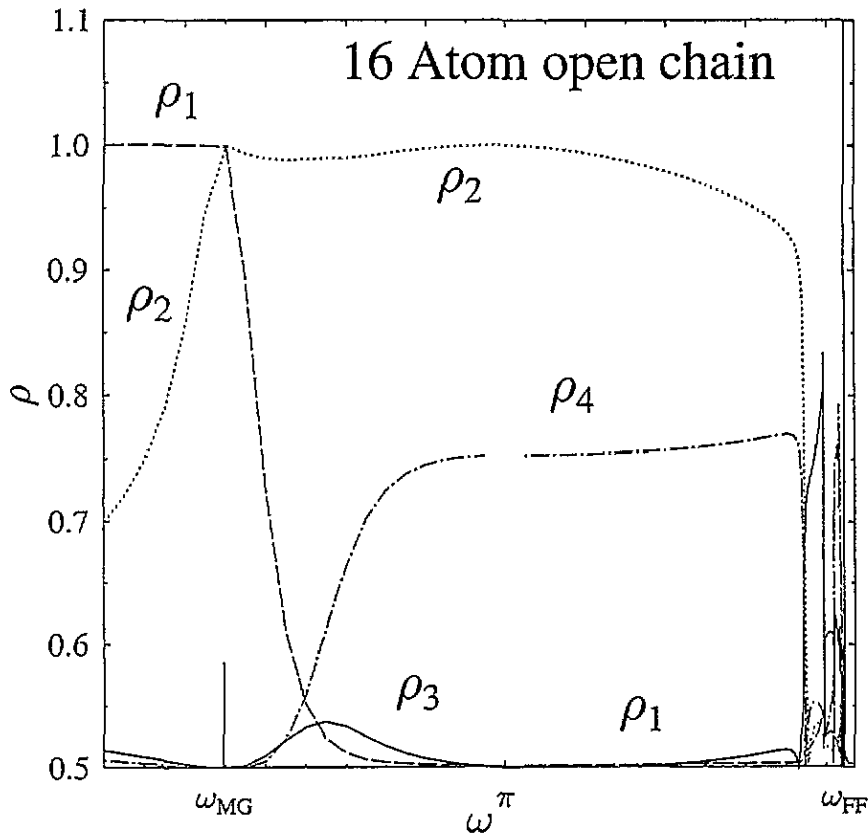


Figure 6. Marshall sign parameters ρ_i as a function of ω .

ρ_3 at $\omega \approx 2.82$ and 2.85 are caused by the crossing of a quintuplet state to become the ground state between these two values. This may be a 'small- N ' effect, although even here ρ_3 is larger than the other ρ_i . Finally, we observe a region closer to ω_{FF} in which ρ_4 is the largest. Results in this area are difficult to obtain because there are many states lying close to the ground state and convergence is extremely slow.

Nevertheless, these results do suggest that the periodicity in the frustrated regime increases as the ferromagnetic boundary is approached. At present, the quantum system looks rather different to the classical as the change in periodicity occurs as a sequence of crossovers rather than smoothly. However, the chains are still relatively short and it may well be that in the large- N limit the behaviour would approximate more closely to the classical.

6. Conclusion

The quantum mechanical behaviour of the frustrated phase of this system is clearly rather complex. The picture that is beginning to emerge is that the variation in periodicity with ω that is characteristic of the classical ground state may well survive partially in the quantum system. However, there are clearly many differences in detail and also some completely new features.

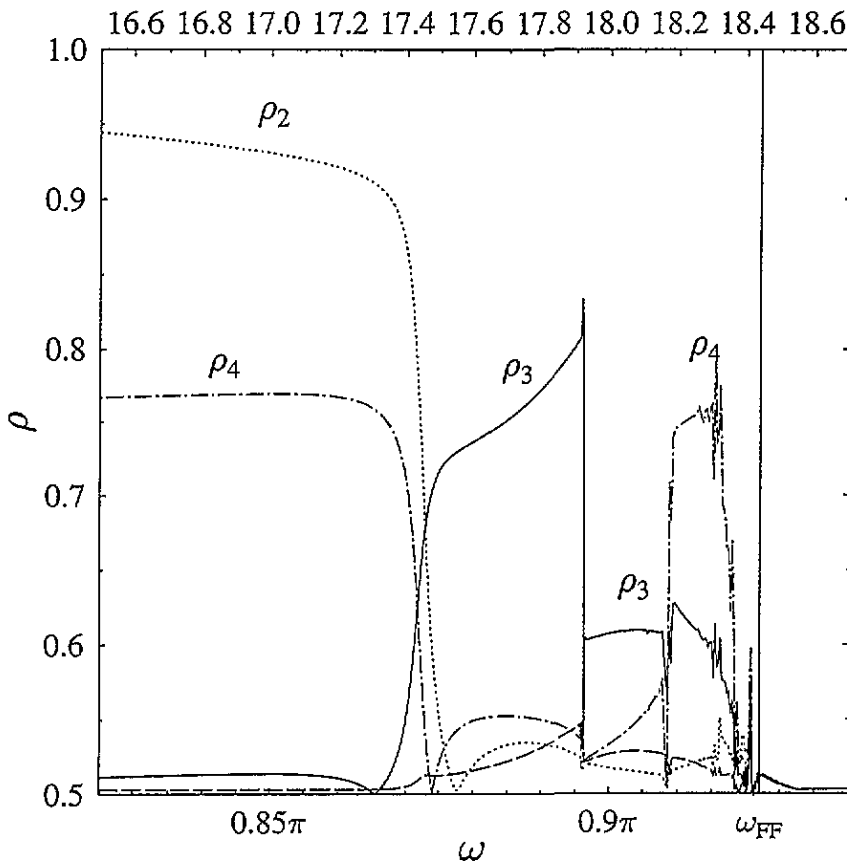


Figure 7. Enlarged part of figure 6 showing region close to ω_2 .

The main difference in detail is that the periodicity of the quantum system, as predicted by the coupled-cluster method and the variational method and confirmed by the DMRG results, remains closer to $\pi/2$ over a much wider range of ω than does the classical system. Another difference, suggested by the Marshall sign calculations, is that the changes in periodicity close to the ferromagnetic boundary may occur less smoothly.

The behaviour of the quantum system close to the Majumdar–Ghosh point is quite different, as there is no classical analogue of the highly dimerized nature of the ground state.

Acknowledgments

We have benefited greatly from discussions with R F Bishop and Yang Xian. DJJ Farnell acknowledges a postgraduate award from the Science and Engineering Research Council of Great Britain. R Bursill is supported by SERC, under grant GR/J26748.

Appendix 1. Solution of the full SUB2 equations

The full SUB2 equations (3.1) can be solved using Fourier transforms as described in

Appendix A of I. The result is

$$b_r = \frac{1}{\pi} \int_0^\pi dq \cos(rq) \Gamma(q) \quad (\text{A1.1})$$

with $\Gamma(q)$ given by

$$\alpha \Gamma(q)^2 + \beta \Gamma(q) + \gamma = 0 \quad (\text{A1.2})$$

where

$$\alpha = J_1 \cos(q) [\cos(\theta) - 1] + J_2 \cos(2q) [\cos(2\theta) - 1]$$

$$\beta = J_1 \{B_1 + 2 \cos(q) [\cos(\theta) + 1]\} + J_2 \{B_2 + 2 \cos(2q) [\cos(2\theta) + 1]\}$$

$$\begin{aligned} \gamma = J_1 \{ & A_1 \cos(q) - 2b_1 [\cos(\theta) + 1] + [1 - \cos(\theta)] X_1 \} \\ & + J_2 \{ A_2 \cos(2q) - 2b_2 [\cos(2\theta) + 1] + [1 - \cos(2\theta)] X_2 \} \end{aligned}$$

where

$$X_1 = \sum_s b_s b_{s+1} \quad X_2 = \sum_s b_s b_{s+2}.$$

These equations are then solved numerically by constructing self-consistency equations in the coefficients b_1 and b_2 and also X_1 and X_2 . Again θ is varied to find the minimum E_g .

References

- Bishop R F, Parkinson J B and Xian Yang 1991 *Phys. Rev. B* **44** 9425
 Bursill R J, Xiang T and Gehring G A 1995 *J. Phys. A: Math. Gen.* **28** 2109
 Chitra R, Pati S K, Krishnamurthy H R, Sen D and Ramasesha S 1994 DMRG studies of the spin-half Heisenberg system with dimerization and frustration *Preprint*
 Farnell D J J and Parkinson J B 1994 *J. Phys.: Condens. Matter* **6** 5521
 Haldane F D M 1982 *Phys. Rev. B* **25** 4925
 Majumdar C K and Ghosh D K 1969a *J. Math. Phys.* **10** 1388
 — 1969b *J. Math. Phys.* **10** 1399
 Marshall W 1955 *Proc. R. Soc. A* **232** 48
 Nomura K and Okamoto K 1992 *Phys. Lett.* **169A** 433
 — 1993 *J. Phys. Soc. Japan* **62** 1123
 — 1994 *J. Phys. A: Math. Gen.* **27** 5773
 Schollwöck U, Jolicoeur Th and Garel T 1995 Physical meaning of the Hückel-Kennedy-Tabas = quantum spin chain *Preprint*
 Tonegawa T and Harada I 1987 *J. Phys. Soc. Japan* **56** 2153
 White S R 1992 *Phys. Rev. Lett.* **69** 2863
 — 1993 *Phys. Rev. B* **48** 10345
 White S R and Huse D A 1993 *Phys. Rev. B* **48** 3844
 White S R and Noack R 1992 *Phys. Rev. Lett.* **68** 3487
 Zeng Chen and Parkinson J B 1995 *Phys. Rev. B* **51** 11609